Environmental Prediction in Canadian Cities - EPiCC
EPiCC Technical Report No. 1

Ben Crawford, Andreas Christen, Rick Ketler

Processing and Quality Control Procedures of Turbulent Flux Measurements during the Vancouver EPiCC Experiment

a place of mind
THE UNIVERSITY OF BRITISH COLUMBIA

EPiCC
Environmental Prediction in Canadian Cities

Cite this report as:

Crawford B., Christen A., Ketler R. (2013): 'Processing and quality control procedures of turbulent flux measurements during the Vancouver EPiCC experiment'. EPiCC Technical Report No. 1, Technical Report of the Department of Geography, University of Britisch Columbia.
http://circle.ubc.ca/, 28pp, Version 1.1

Cover Photo: Flux Tower 'Vancouver Oakridge' in Summer 2009. Photo by A. Christen

The research network 'EPiCC' was supported by the Canadian Foundation for Climate and Atmospheric Sciences (CFCAS)

Environmental Prediction in Canadian Cities

CFCAS Network 2006-2010

EPiCC Technical Report No. 1

Processing and quality control procedures of turbulent flux measurements during the Vancouver EPiCC experiment

Ben Crawford, Andreas Christen and Rick Ketler

Department of Geography, University of British Columbia

Version 1.1

February 2012

Introduction

This report summarizes data processing and quality control procedures used during the Vancouver experiment of the Environmental Prediction in Canadian Cities (EPiCC) network in 2007-2010. The document describes the procedures applied to calculate turbulent fluxes of sensible heat, latent heat and carbon dioxide. Turbulent fluxes were measured at two suburban sites and one rural reference site (Figure 1). Symbol definitions and units used in this report are found in Table 9.

As part of the EPiCC Network, the University of British Columbia / Department of Geography monitored energy, water, and carbon balances in two suburban neighborhoods in Vancouver, BC, Canada in 2008-2009. Two flux towers, 'Vancouver-Sunset' and 'Vancouver-Oakridge', were operated in extensive residential areas composed of single-family homes. A rural reference flux station 'Westham Island' was located on flat, unmanaged and non-irrigated grassland 16 km south of the two urban neighborhoods in an area dominated by intensive farming.

Instrumentation

Turbulent fluxes (latent heat flux (Q_E), sensible heat flux (Q_H), and carbon dioxide flux (F_C) were measured at all three sites using Campbell Scientific CSAT-3d sonic anemometers and open-path Li-COR Li-7500 infrared gas analyzers (IRGAs) using the eddy-covariance method. Wind direction (*u*, *v*, and *w* components), acoustic air temperature (T_A), and CO_2 (*c*) and H_2O (*q*) concentrations were sampled continuously at 20 Hz.

Figure 1. *Photos of the eddy-covariance systems at Vancouver-Sunset, Vancouver Oakridge, and Westham Island.*

Table 1. *Set-up and settings of ultrasonic anemometer-thermometers used during EPiCC.*

Site	**Sensor height above ground** (m)	**Azimuth**[1] (º)	**Sensor model**	**Serial number**	**Wicks**	**Settings**
Vancouver-Sunset (ST)	28.8	179.1	Campbell Scientific CSAT 3D	**1394** (6/5/2008 – 4/6/2009) **1342** (4/6/2009 onward)	Yes	60 Hz internal, 20 Hz output (SDM)
Vancouver-Oakridge (OM)	29	305.0 (2008) 321.6 (2009)	Campbell Scientific CSAT 3D	**1393**	Yes	60 Hz internal, 20 Hz output (SDM)
Westham Island (WI)	1.8 (27/7/2007 – 23/6/2009) 2.2 (23/6/2009 – 8/10/2009)	355.0	Campbell Scientific CSAT 3D	**1342** (27/7/2007 – 4/6/2009) **1393** (4/6/2009 – 11/6/2009) **1394** (11/6/2009 – 8/10/2009)	Yes	60 Hz internal, 20 Hz output (SDM)

Table 2. *Set-up of infrared gas analyzers used during EPiCC.*

Site	**Sensor height above ground** (m)	**Azimuth relative to Sonic** (º)	**Distance to sonic** (Vertical, Horizontal cm)	**Tilt from vertical**	**Sensor models used**
Vancouver-Sunset	28.8	Approx. 300º	0, 40	Tilted approx. 60º to South	**1222** (6/5/2008 – 24/6/2009) **0561** (24/6/2009 – present)
Vancouver-Oakridge	29	Approx. 60º	0, 18	Tilted approx. 30º to North	**0561** (8/7/2008 – 27/8/2008) **1222** (27/6/2009 – 31/8/2009)
Westham Island	1.8 (27/7/2007 – 23/6/2009) 2.2 (23/6/2009 – 8/10/2009)	Approx. 350º	0, 17	Tilted approx 60º to North	**0151** (27/7/2007 – 10/10/2008) **0561** (10/10/2008 – 23/6/2009) **0151** (23/6/2009 – 8/10/2009)

[1] Direction the sensor head is facing towards as seen from the level / mount relative to Geographic North.

Sensor Calibrations

As part of an NSERC DG research program, a field intercomparison of sonic anemometers was conducted from May 27 – June 15, 2009 at the Westham Island site including sonics used during EPiCC. Results for the sonics that were operated during EPiCC are summarized in Appendix 1 (Table 6). Although sonic SN#1342 was involved in the intercomparison, there are no statistics available for SN#1342 because there were no 30-minute periods deemed acceptable for comparison (i.e. greater than 90% of measured wind direction from 45° in front of the sonic).

Figure 3. *Intercomparison set-up close to the the Westham Island site.*

The IRGAs were calibrated regularly in the UBC Biometeorology lab (Table 3). First, H_2O and CO_2 readings are zeroed using dry N_2 gas with 0 ppm CO_2. Next, the H_2O readings are spanned with air at a dew point temperature of 8.5° C using a dew point generator. Finally, CO_2 is spanned using reference gas of 452 ppm CO_2.

Table 3. *Calibrations and software settings of infrared gas analyzers used during EPiCC.*

Model	**Serial No**	**Calibration Dates**	**OS Version** during EPiCC
LI-7500	**0151**	5/12/2007, 23/10/2008, 10/6/2009	Windows Interface v3.0.2 Internal v3.0.1
LI-7500	**0561**	26/6/2008, 24/6/2009	Windows Interface v3.0.2 Internal v3.0.1
LI-7500	**1222**	4/3/2008, 15/6/2009	Windows Interface v3.0.2 Internal v3.0.1

High frequency quality control

In a first step, high frequency (20 Hz) data pass through several quality control filters before covariances and fluxes are calculated:

Sonic anemometer diagnostic value

The CSAT sonic anemometer reports if the sonic anemometer path is obstructed, the path length has been altered, or for up to 10 seconds after the sonic has just been powered on (Campbell Scientific, 2009). Individual high frequency *u*, *v*, *w*, and *t* data points are withheld from further processing when diagnostic values are triggered.

IRGA diagnostic value

Precipitation, condensation, fog, insects, etc. in the optical path of the IRGA may interfere with measurements of *c* and *q*. The automatic gain control (AGC) output of the IRGA registers a change in value if the optical path of the IRGA is blocked (LI-COR, 2004). The AGC value was recorded at 20 Hz at all sites and ranges from 0 – 100 (the optical path is completely obscured at 100). If there is any change in AGC value, or if the AGC value is greater than 90, H_20 and CO_2 high frequency data for ±5 seconds around that point are withheld from further processing.

High frequency spike detection

Random electronic noise and short-term data 'spikes' are filtered out of high frequency data sets using a dynamic iterative standard deviation filter (e.g. Vickers and Mahrt 1997). First, individual 20 Hz data points are flagged if they fall outside a physically justified, realistic data range for each variable (Table 5). Individual 20 Hz data points are then flagged as spikes and withheld from further processing if they are above or below a variable-specific standard deviation threshold from a 30-minute mean (Table 5). Consecutive passes are then performed with the standard deviation threshold raised by 0.3 each time until no spikes are detected. Spikes must also be less than 0.3 seconds in duration, otherwise they are considered real.

Flow distortion by the sensor head

Wind tunnel measurements of CSAT-3d anemometers show that flow is strongly distorted when ± 7º from directly behind the sonic mounting block (Figure 4). 30-minute flux averaging periods are flagged as questionable if more than 25% of 20 Hz wind directions fall within ± 7º of 180º from the sonic's azimuth (Table 4).

Table 4. *Wind directions influenced by sonic anemometer mounting block. The Oakridge Tower sonic anemometer was oriented differently during 2008 and 2009.*

Site	Wind directions withheld from flux processing
Vancouver-Sunset	352° - 6°
Vancouver-Oakridge	118°- 132° (2008), 134.6° - 148.6° (2009)
Westham Island	168° - 182°

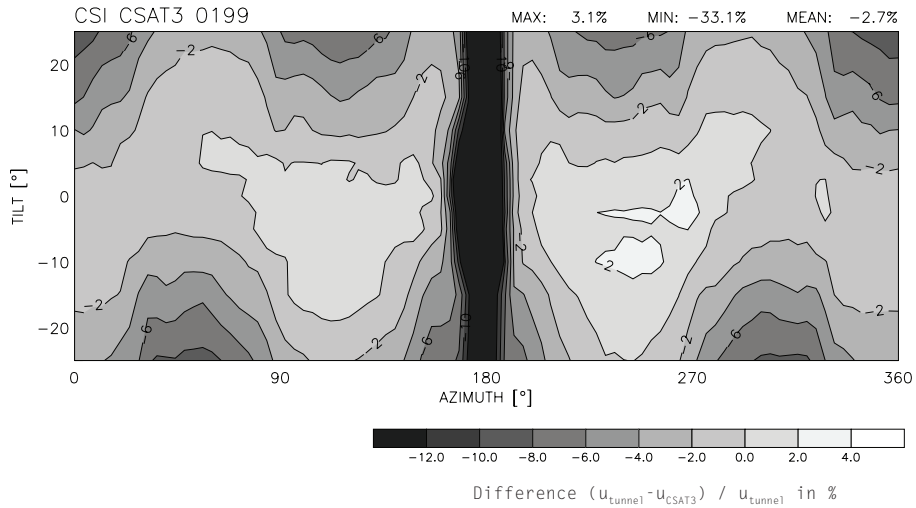

Figure 4. *Difference of wind speed measurement (vector mean) between wind tunnel and a CSAT3d sonic anemometer at 4 m s^{-1} dependent from azimuth and tilt in % (Christen et al., 2002).*

High-frequency statistics check

Statistics of 30-minute standard deviation, skewness, and kurtosis are calculated for *u*, *v*, *w*, *t*, *q*, and *c*. Empirical limits were determined for each variable and data from periods with values outside these limits are flagged as questionable (Table 5).

Table 5. *Summary of quality control limits and thresholds used for high-frequency eddy covariance data.*

	u (m s^{-1})	**v (m s^{-1})**	**w (m s^{-1})**	**t (°C)**	**q (mmol m^{-3})**	**c (mmol m^{-3})**
Physically-based min/max thresholds (variable units)	-30 / 30	-30 / 30	-5 / 5	-20 / 40	100 / 1500	12 / 40
Spike threshold (standard deviations)	6	6	8	8	10	10
Standard deviation (min/max)	0.05 / 4.0	0.05 / 4.0	0.02 / 1.5	0.01 / 2.0	0.01 / 150.0	0.001 / 2.0
Skewness (min/max)	-3.0 / 3.0	-3.0 / 3.0	-2.0 / 2.0	-2.5 / 2.5	-5.0 / 5.0	-5.0 / 5.0
Kurtosis (min/max)	-2.0 / 5.0	-2.0 / 5.0	-2.0 / 15.0	-2.0 / 15.0	-2.0 / 15.0	-2.0 / 15.0

Sonic – IRGA time lag

Due to the separation of the sonic anemometer and IRGA, measurements of *q* and *c* are not exactly correlated with measurements of wind velocity because of the travel time of an air parcel between the sonic and IRGA. The magnitude of this lag was calculated by shifting *q* and *c* time series relative to *w* and determining the maximum covariance (Table 6). Lag times vary by wind direction and were calculated for eight wind sectors at each site, but only average lag times are reported here.

Table 6. *Average sonic – IRGA lag in milliseconds and number of records by site and IRGA for both CO_2 and H_2O.*

Site and Date	IRGA SN	CO_2 (ms)	CO_2 (records)	H_2O (ms)	H_2O (records)
ST					
6/5/2008 – 23/6/2009	1222	-42.1	-0.84	-41.1	-0.82
25/6/2009 – 20/4/2010	0561	-41.8	-0.84	-40.0	-0.80
OM					
9/7/2008 – 31/8/2008	0561	-30.7	-0.61	-31.2	-0.62
27/6/2009 – 31/8/2009	1222	-32.8	-0.66	-25.4	-0.50
WI					
27/7/2007 – 31/12/2008	0151	7.2	0.14	-5.29	-0.11
11/10/2009 – 23/6/2009	0561	20.76	0.42	12.99	0.25
24/7/2009 – 8/10/2009	0151	-38.1	-0.76	-44.3	-0.89

For all sites, lag times were less than the 20 Hz measurement resolution (i.e. less than 1 record length), so it is doubtful that the lag can be accounted for by shifting the sonic and IRGA time-series relative to each other with out introducing additional uncertainties. To test this, covariances (*w'c'* and *w'q'*) were calculated with IRGA *c* and *q* time series shifted forward by 1 record length relative to the sonic wind vector data. These covariances were then compared with covariances calculated from un-shifted data. Seven half-hour periods (20 July 2009, 0900-1200) measured at Sunset Tower were used as a test period representative of summer, clear sky conditions with flow from the NW. Covariances calculated from shifted time series were 0.4% different for *w'c'* and 0.3% different for *w'q'* than un-shifted covariances. This difference is deemed negligible, so record-shifting is not implemented during flux data processing.

Block average calculation and rotation

In a second step after initial high frequency data quality control filters, mean values and higher-order moments (including covariances) are calculated if a 30-minute period has greater than 75% of possible *u*, *v*, *w*, T_A, *c*, and *q* 20 Hz data points.

Wind components are rotated two times so that the *x*-axis of the new sonic coordinate system is aligned with the mean 30-minute wind direction, and the mean vertical wind *w* is zero (e.g. McMillen 1988, Finnigan et al. 2002). Following Reynold's decomposition, 30-minute statistics are calculated based on a simple block-average.

Corrections applied to turbulent flux densities

30-minute fluxes are then subject to additional corrections and quality control filters specific to Q_H, Q_E and F_C.

Latent Heat Flux (Q_E)

1) The 30-minute QE is calculated as:

$$Q_E = L_V * \overline{w'q'} \quad [1]$$

where:

$$L_V = (2.501 - 0.00237 * T) * 10^6 \quad [2]$$

2) Q_E values are then corrected to account for volume and density changes of air due to temperature and water vapor fluctuations. Following Webb et al. (1980), the corrected Q_E is:

$$Q_E = \overline{w'q'} + \frac{M_A}{M_q} * \frac{\rho_q}{\rho_A} * \overline{w'q'} + \left(1 + \frac{M_A}{M_q} * \frac{\rho_q}{\rho_A}\right) * \frac{\rho_q}{T_A} * \overline{w't'} \quad [3]$$

where:

$$\rho_q = \frac{e * M_q}{T * R} \quad [4]$$

and:

$$\rho_A = \frac{(P - e) * M_A}{T * R} \quad [5]$$

and based on the Clausius-Clapeyron equation:

$$e = RH * \left[e_O * \exp\left(\frac{L_V}{R_V} * \left(\frac{1}{273} - \frac{1}{T}\right)\right)\right] \quad [6]$$

3) Q_E values are also corrected to account for high frequency flux losses based on IRGA and sonic anemometer path length and separation between the IRGA and sonic anemometer sensors (Moore 1986). Inputs to the Moore correction include:

- Instrument specific path lengths of the sonic (11.6 cm) and IRGA (12.5 cm)
- Site specific sonic and IRGA horizontal separation (Table 2).
- Measurement height (Table 1).
- Measured horizontal wind speed from sonic anemometer.
- Zero-plane displacement (z_d), estimated as 2/3 the average height of the canopy (effective canopy height = 10.6 m for Sunset, 8.0 m for Oakridge, variable canopy height at Westham because of growing grass (Figure 5)).
- Monin-Obukhov Length, calculated as:

$$L = -1 * \frac{\left(\left((\overline{u'w'})^2 + (\overline{v'w'})^2\right)^{0.25}\right)^3}{k * \left(\frac{g}{T}\right) * \overline{w't'}} \quad [7]$$

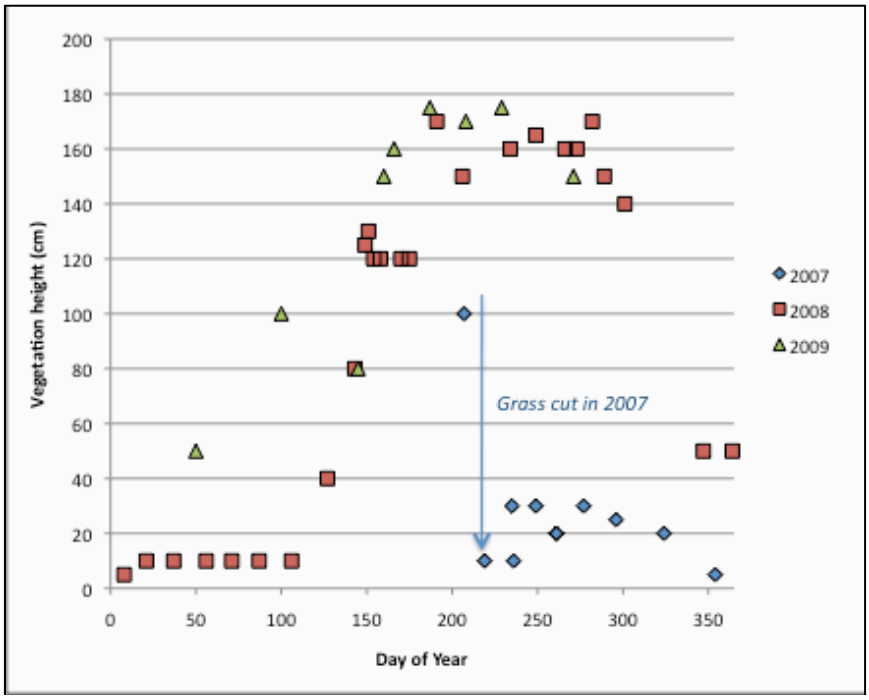

Figure 5. *Vegetation canopy height at Westham Island used as an input to the Moore flux correction.*

4) Comparisons of potential temperature measured from both the sonic anemometer and HMP T/RH sensor at each site were used as a check on sonic performance. During and after precipitation events when the sonic path length may be obstructed by water, measurements of wind velocities (and therefore Q_E) may be unreliable. During these periods, the HMP's ability to measure temperature is assumed to be unaffected.

For each site and sonic, potential temperature was calculated from the sonic and HMP temperature measurements and compared. If the difference between measurements fell outside of empirically determined limits for each site/sensor configuration, 30-minute values of Q_E were flagged as questionable (Table 7).

Sensible Heat Flux (Q_H)

1) 30-minute Q_H is calculated as:

$$Q_H = \overline{w't'} * c_p * \rho \quad [8]$$

where

$$c_p = 1004.67 * (1 + 0.84 * r) \quad [9]$$

and

$$r = \frac{0.622 * e}{P - e} \quad [10]$$

2) Q_H values are then corrected to account for moisture influences on air temperature and density. Following Schotanus et al. (1983), corrected Q_H is:

$$Q_H = \overline{w't'} - 0.51 * \left(\frac{T_A}{1 + 0.51 * \rho_q} \right) * \overline{w'q'} \quad [11]$$

3) Q_H values are also corrected to account for high frequency flux losses based on sonic anemometer acoustic path length (Moore 1986, refer also to Q_E section).

4) Comparisons of potential temperature measured from both the sonic anemometer and HMP T/RH sensor at each site were used as a check on sonic performance. During and after precipitation events when the sonic path length may be obstructed by water, measurements of wind velocities and temperature (and therefore Q_H) may be unreliable. During these periods, the HMP's ability to measure temperature is assumed to be unaffected.

For each site and sonic, potential temperature was calculated from the sonic and HMP temperature measurements and compared. If the difference between measurements fell outside of empirically determined limits for each site/sensor configuration, 30-minute values of Q_H were flagged as questionable (Table 7).

Carbon Dioxide Flux (F_C)

1) 30-minute F_C is calculated as:

$$F_C = \overline{w'c'} \quad [12]$$

2) F_C values are then corrected according to Webb et al. (1980):

$$F_C = \overline{w'c'} + \frac{M_A}{M_q} * \frac{\rho_C}{\rho_A} * \overline{w'q'} + \left(1 + \frac{M_A}{M_q} * \frac{\rho_q}{\rho_A} \right) * \frac{\rho_C}{T_A} * \overline{w't'} \quad [13]$$

3) F_C values are also corrected to account for high frequency flux losses based on IRGA and sonic anemometer path length and horizontal separation between the IRGA and sonic anemometer sensors (Moore 1986, refer also to Q_E section).

4) Comparisons of potential temperature measured from both the sonic anemometer and HMP T/RH sensor at each site were used as a check on sonic performance. During and after precipitation events when the sonic

path length may be obstructed by water, measurements of wind velocities (and therefore F_C) may be unreliable. During these periods, the HMP's ability to measure temperature is assumed to be unaffected.

For each site and sonic, potential temperature was calculated from the sonic and HMP temperature measurements and compared. If the difference between measurements fell outside of empirically determined limits for each site/sensor configuration, 30-minute values of F_C were flagged as questionable (Table 7).

5) Hourly CO_2 storage (ΔF_S) below measurement height was accounted for using half-hourly changes in CO2 concentration measured by the IRGA at the height of the eddy-covariance system:

$$\Delta F_S = z \cdot \Delta c$$

where *z* is the measurement height (effectively, this is the air column volume below measurement height in m^3), Δc is the change in CO_2 concentration (µmol m^{-3} s^{-1}) (Hollinger *et al*., 1994).

Table 7. *Sonic – HMP quality control temperature departure limits.*

Site and Date	Sonic SN	Low/High limit (°C)
ST		
06/05/2008 – 04/06/2009	1394	-1.5 / 1.5
04/06/2009 - present	1342	-1.5 / 1.5
OM		
30/06/2008 – 31/08/2009	1393	-1.5 / 1.5
WI		
01/07/2007 - 11/06/2009	1394	-1.5 / 1.5
11/06/2009 – 08/10/2009	1394	-2.0 / 2.0

Table 8*. IRGA – HMP quality control specific humidity departure limits.*

Site and Date	IRGA SN	Low/High limit (g kg^{-1})
ST		
06/05/2008 – 24/06/2009	1222	-0.75 / 0.75
24/06/2009 – 18/03/2010	0561	-0.75 / 0.75
OM		
30/06/2008 – 27/8/2008	0561	-0.75 / 0.75
27/6/2009 – 31/8/2009	1222	-0.75 / 0.75
WI		
01/07/2007 - 10/10/2008	0151	-3 / 3
10/10/2008 – 23/6/2009	0561	-1.5 / 1.5
23/6/2009 – 8/10/2009	0151	-3 / 3

Table 9. *Symbol definitions and units.*

Symbol	Definition	Units	Value
Q_E	Turbulent latent heat flux density	W m^{-2}	
Q_H	Turbulent sensible heat flux density	W m^{-2}	
F_C	Turbulent carbon dioxide flux density	µmol m^{-2} s^{-1}	
u	Longitudinal wind component	m s^{-1}	
v	Lateral wind component	m s^{-1}	
w	Vertical wind component	m s^{-1}	
T	Air temperature from slow-response sensor	K	
T_A	Acoustic air temperature from sonic anemometer	K	
c	Atmospheric carbon dioxide concentration	µmol m^{-3}	
q	Atmospheric water vapor concentration	g m^{-3}	
$\overline{w'q'}$	Covariance of *w'* and *q'*	g m^{-2} s^{-1}	
$\overline{w't'}$	Covariance of *w'* and *t'*	K m s^{-1}	
$\overline{w'c'}$	Covariance of *w'* and *c'*	µmol m^{-2} s^{-1}	
L	Obukhov length	m	See equation [4]
k	Von-Karman constant		0.4
g	Gravitational acceleration	m s^{-2}	9.8
L_V	Latent heat of vaporization	J kg^{-1}	See equation [2]
M_A	Molecular mass of dry air	kg mol^{-1}	0.02896
M_q	Molecular mass of water vapor	kg mol^{-1}	0.01802
ρ_A	Density of dry air	kg m^{-3}	See equation [5]
ρ_q	Density of water vapor	kg m^{-3}	See equation [4]
ρ_C	Density of carbon dioxide	kg m^{-3}	
ρ	Density of moist air	kg m^{-3}	$\rho_A + \rho_q$
e	Vapor pressure	hPa	See equation [6]
r	Mixing ratio	kg kg^{-1}	See equation [10]
R	Universal gas constant	J K-1 mol-1	8.314
R_V	Gas constant for water vapour	J K-1 kg-1	461
RH	Relative humidity	%	
P	Barometric pressure	hPa	
c_p	Specific heat of air	J kg^{-1} K^{-1}	See equation [9]
Q^*	Net all-wave radiation	W m^{-2}	
ws	Wind speed	m s^{-1}	

Appendix 1 – Sonic Anemometer-Thermometer Field Intercomparison

Table 10. *Summary of results from the sonic anemometer field intercomparison expressed as linear regression between measured value and reference sonic value (#1389)*

Parameter	Sonic SN	Slope	Intercept	Mean difference from reference	Std. dev. of difference from reference	Reference mean (SN# 1389)
Mean u (m s^{-1})	1393	0.99749	-0.00297	-0.00876	0.04878	2.39409
	1394	1.00429	-0.00440	0.00631	0.04173	
Mean v (m s^{-1})	1393	0.98079	0.02516	0.01870	0.02655	0.34126
	1394	1.00879	-0.10279	-0.09941	0.03136	
Mean w (m s^{-1})	1393	-0.08958	-0.01906	-0.01712	0.01868	-0.00179
	1394	0.28074	-0.05172	-0.05126	0.01637	
Mean T (C)	1393	1.01565	0.48876	0.72420	0.04658	15.04097
	1394	0.99663	1.41406	1.36362	0.05507	
3d vector wind (m s^{-1})	1393	0.99799	-0.00313	-0.00797	0.04529	2.46384
	1394	1.00121	-0.00767	-0.00458	0.05141	
3d cup wind (m s^{-1})	1393	0.99891	-0.00574	-0.00846	0.04227	2.59927
	1394	1.00280	-0.01015	-0.00256	0.04919	
u'u' (m^{-2} s^{-2})	1393	1.02985	-0.00901	0.01121	0.03736	0.70542
	1394	1.00395	0.00110	0.00409	0.04711	
u'w' (m^{-2} s^{-2})	1393	0.99989	-0.00033	-0.00031	0.01078	-0.11404
	1394	1.03891	-0.00080	-0.00559	0.01232	
v'v' (m^{-2} s^{-2})	1393	0.97068	0.00480	-0.00995	0.01933	0.51080
	1394	1.02711	-0.00231	0.01242	0.02494	
v'w' (m^{-2} s^{-2})	1393	0.93731	0.00351	0.00505	0.00896	-0.02230
	1394	1.00223	0.00182	0.00176	0.00762	
w'w' (m^{-2} s^{-2})	1393	1.01042	0.00046	0.00233	0.00643	0.18711
	1394	1.02871	-0.00008	0.00571	0.00819	
w'T' (K m^{-1} s^{-1})	1393	1.03152	0.00012	0.00039	0.00409	0.009561
	1394	1.03336	-0.00040	-0.00009	0.00479	
T'T' (K^2)	1393	1.00606	0.00111	0.00184	0.00937	0.12582
	1394	1.00851	-0.00102	-0.00004	0.00983	
Skew u	1393	0.90993	0.03891	0.01397	0.07393	0.27496
	1394	0.82419	0.06935	0.02226	0.09121	
Skew v	1393	0.95072	0.02620	0.02384	0.06831	0.04972
	1394	0.88830	0.00365	-0.00324	0.08427	
Skew w	1393	0.96794	-0.00615	-0.01354	0.08097	0.13024
	1394	0.63227	0.01794	-0.03138	0.06079	
Skew T	1393	0.98517	-0.00553	-0.00527	0.06234	-0.03131
	1394	0.94224	-0.02531	-0.02296	0.09481	
TKE (m^2 kg^{-1} s^{-2})	1393	1.04064	-0.01425	0.00549	0.05744	0.55195
	1394	1.04542	-0.01115	0.01627	0.06155	

Appendix 2 – Comparison of post-processing software

Appendix 2 compares output from the EPiCC eddy-covariance data processing code developed and used at UBC Geography (ubc_mmd.app, Version 3.04, EPiCC version, IDL based processing) against Eddy Pro (3.0) which is distributed by Licor, Inc.

Five weeks of high-frequency data (20 Hz) measured on Sunset Tower were compared (Feb 7 to Mar 23, 2012) were processed using the settings listed in Table 1 and the output of turbulent fluxes of sensible heat, latent heat, and carbon-dioxide.

Eddy covariance data was measured by a separate system consisting of a CSI CSAT-3 ultrasonic anemometer, a Li-7500A (CO2/H2O open path analyzer), and Li-7700 (CH4 open path analyzer, not used here), all operated at 28.7 m above local ground (tower base). The CSAT was pointing with its undisturbed sector towards 206º from geographic North. The sensor separation between the CSAT-3 measurement volume and the Li-7700 was 45 cm horizontal and 7 cm vertical (Li-7700 is higher than CSAT-3 measurement volume) and the Li-7500 was installed to the NE (53º) of the CSAT-3. The sensor separation between the CSAT-3 measurement volume and the Li-7500A was 35 cm horizontal and 0 cm vertical and the Li-7500A was installed to the North (356º) of the CSAT-3 volume. This system was set apart from the tower's long-term system (at 90 cm horizontal and 10 cm vertical distance to the measurement volume of the long-term system).

The period of the comparison was experiencing extensive periods of rain. First, the entire period was compared. Secondly, the analysis was restricted to three dry days, March 6, 00:30 to March 8, 24:00 without rain. From both time frame all valid data was used (Eddy Pro QC = 0, 1 or 2).

Table 11. *Summary of software Settings of the processing output*

	Eddy Pro Settings	**Settings in ubc_mmd.app**
Tilt correction (axis rotation)	Double rotation (v=0, w=0)	Double rotation (v=0, w=0)
Detrending	Block averaging	Block averaging
Time lag compensation	None	None
Despiking	Yes	Iterative, for limits described in this report (Section 'High frequency spike detection'
Statistical tests	Absolute limits, skewness and kurtosis	Absolute limits, skewness and kurtosis with boundaries described in Table 5
Tests for Analyzer Quality	Yes	AGC test for Li-7500A. Only data when signal strength > 20% for Li-7500
Compensations for density fluctuations	Webb-Pearman-Leuning (open path)	Webb-Pearman-Leuning (open path)
Sonic temperature correction for humidity	van Dijk et al. (2004)	Yes (based on Schotanus et al., 1983)
Filtering of flow distortion	None	Remove data from disturbed sector from block average
Angle of attack corrections	Yes	No
Spectral corrections	Yes (standard)	Sensor separation only (Moore, 1986)

Table 12 - *Comparison between fluxes calculated using ubc_mmd.app and Eddy Pro for the full period of February 7 to March 11, 2012 in terms of a linear regression with Slope and r^2, and expressed as median absolute difference (MedAE). Values is brackets are the error estimates relative to the average flux in the given period. Data includes all data that was outputted with various quality flags.*

	Slope	r2	MedAE	MedAE relative to average flux
Sensible heat flux (W m^{-2})	EddyPro = 1.008 * UBC	r^2 = 0.990	0.60 W m^{-2}	2.2%
Latent heat flux (W m^{-2})	EddyPro = 1.038 * UBC	r^2 = 0.960	0.51 W m^{-2}	1.7%
CO_2 Flux (µmol m^{-2} s^{-1})	EddyPro = 1.003 * UBC	r^2 = 0.989	0.30 µmol m^{-2} s^{-1}	1.4%

Table 13 - *Comparison between fluxes calculated using ubc_mmd.app and Eddy Pro for the dry period of March 6 to March 8, 2012 in terms of a linear regression with Slope and r2, and expressed as median absolute difference (MedAE). Values is brackets are the error estimates relative to the average flux in the given period. Data includes all data that was outputted with various quality flags.*

	Slope	r2	MedAE	MedAE relative to average flux
Sensible heat flux (W m^{-2})	EddyPro = 1.015 * UBC	r^2 = 0.999	0.58 W m^{-2}	1.2%
Latent heat flux (W m^{-2})	EddyPro = 1.039 * UBC	r^2 = 0.997	0.63 W m^{-2}	3.2%
CO_2 Flux (µmol m^{-2} s^{-1})	EddyPro = 1.016 * UBC	r^2 = 0.996	0.34 µmol m^{-2} s^{-1}	1.7%

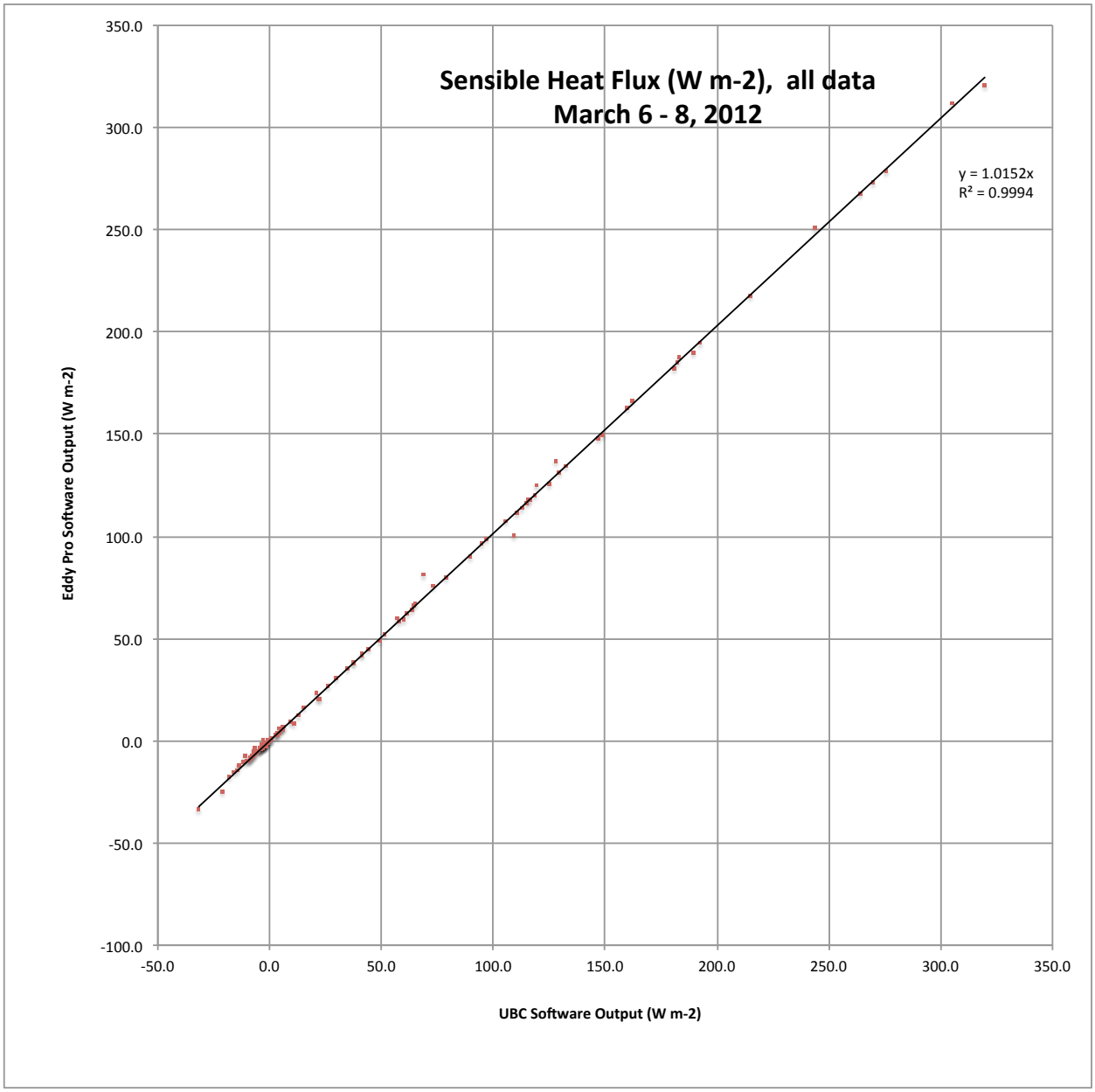

Figure 6 *- Comparison between sensible heat fluxes calculated using ubc_mmd.app and Eddy Pro for the three day period of March 6 to March 8, 2012. Includes all data with QC 0, 1 and 2.*

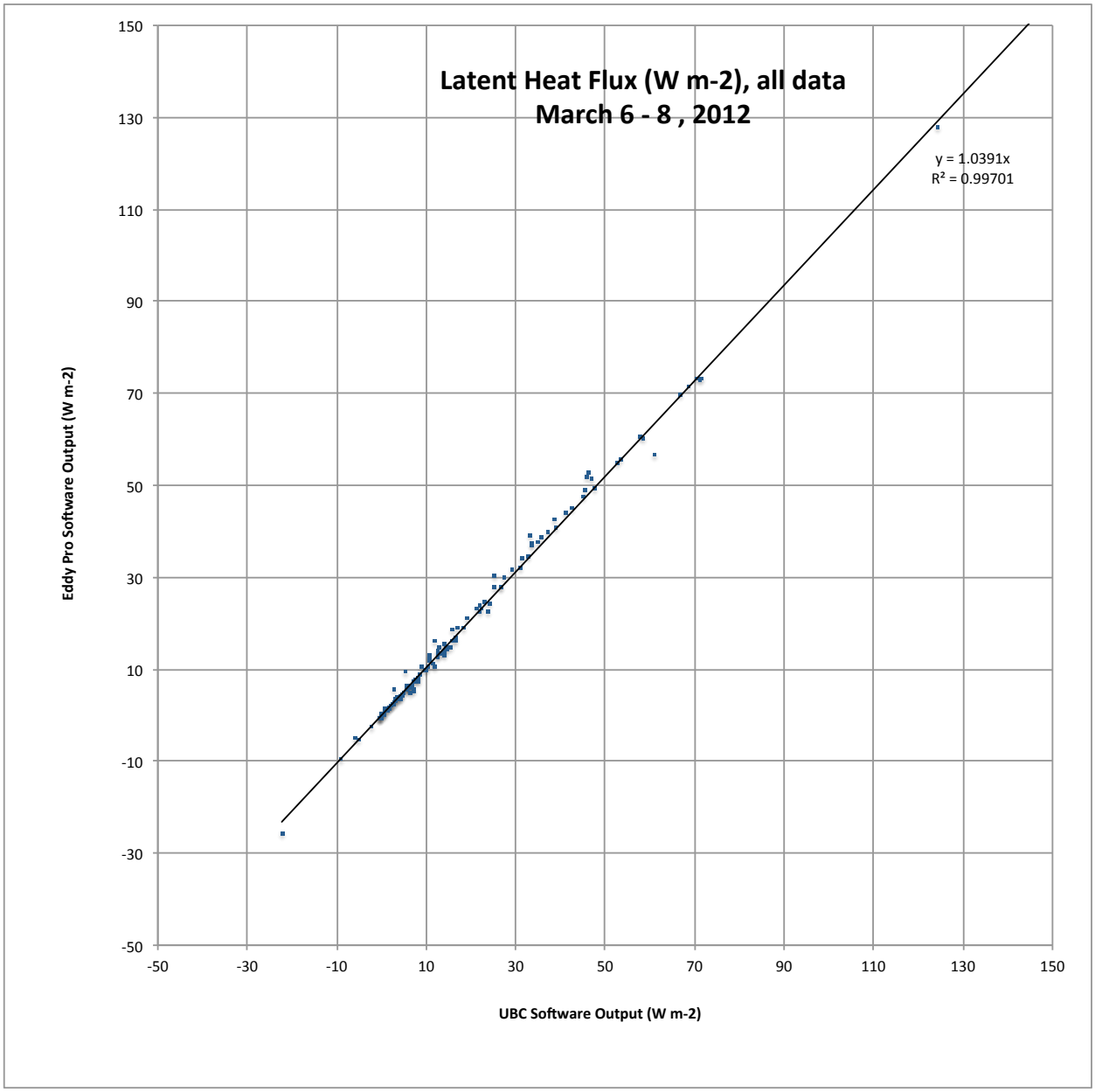

Figure 7 - *Comparison between latent heat fluxes calculated using ubc_mmd.app and Eddy Pro for the three day period of March 6 to March 8, 2012. Includes all data with QC 0, 1 and 2.*

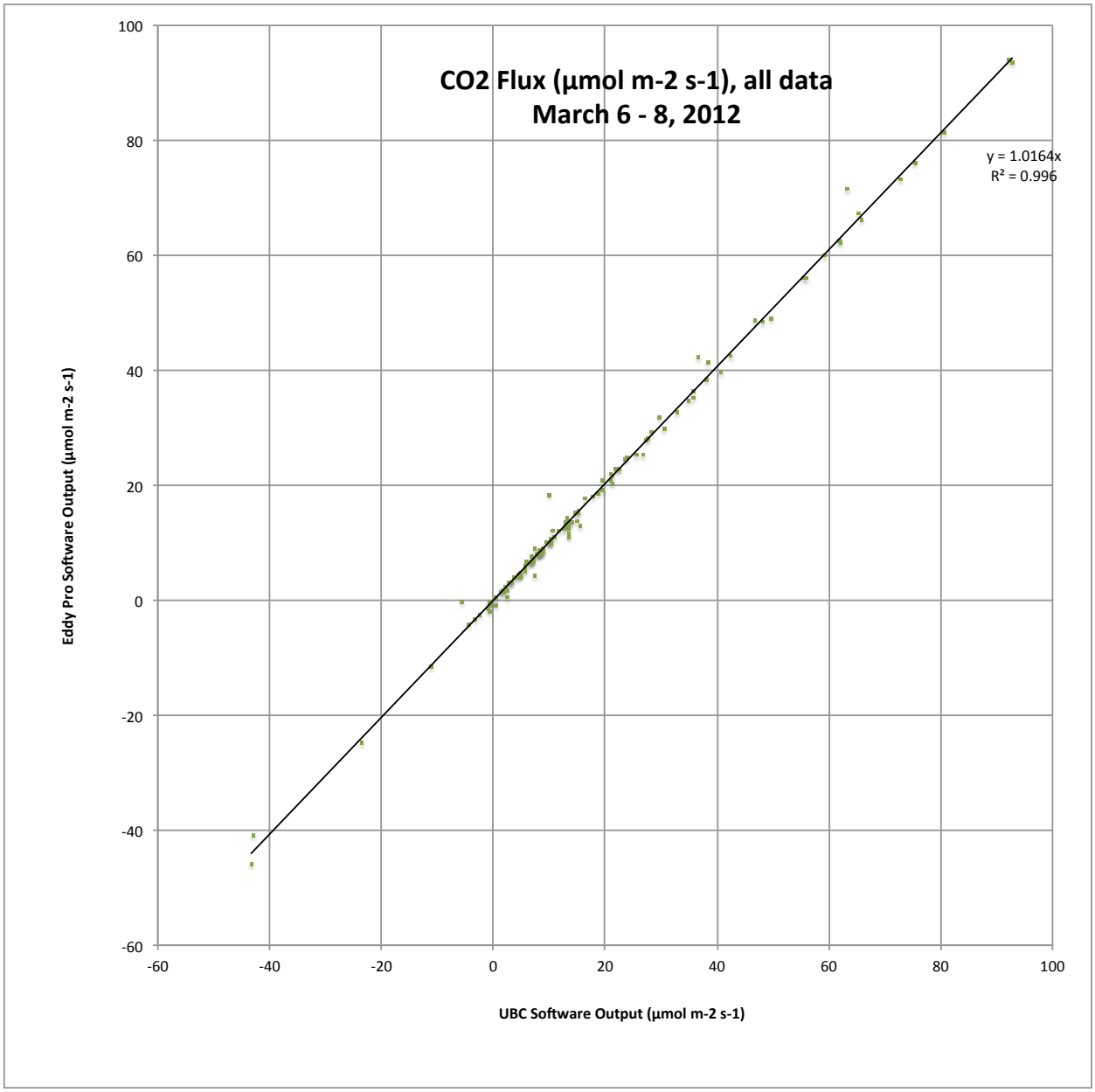

Figure 8 - *Comparison between carbon-dioxide mass fluxes calculated using ubc_mmd.app and Eddy Pro for the three day period of March 6 to March 8, 2012. Includes all data with QC 0, 1 and 2.*

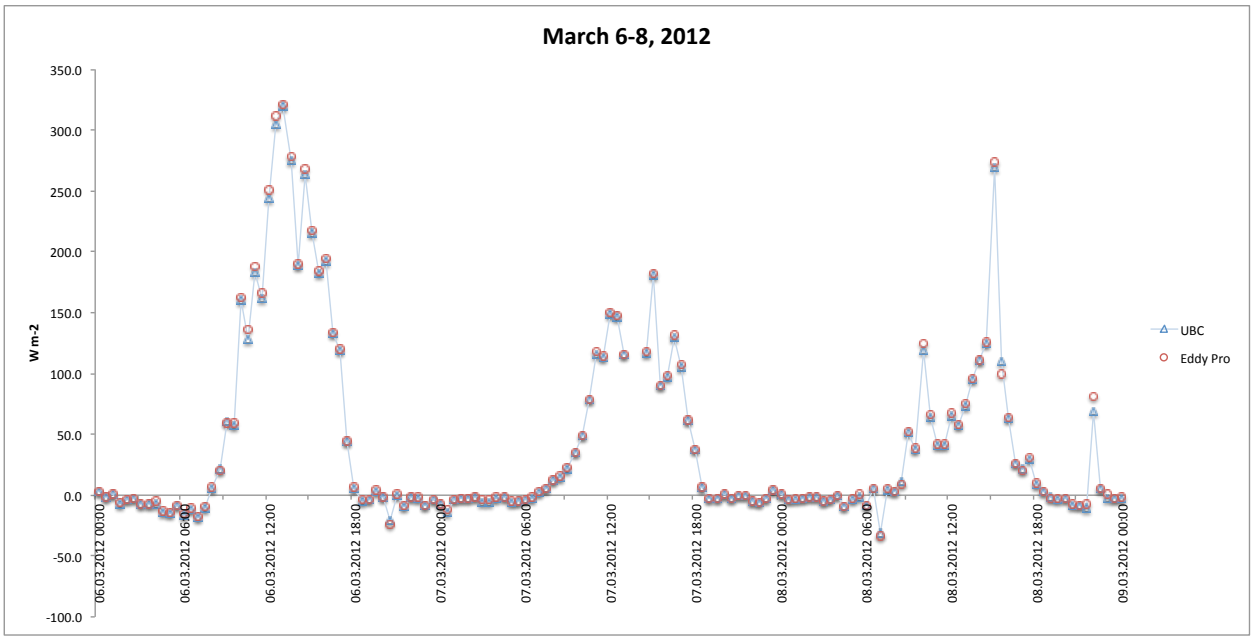

Figure 9 *- Time series of sensible heat flux calculated using ubc_mmd.app (UBC, blue triangles) and Eddy Pro (red circles) for the three day period of March 6 to March 8, 2012.*

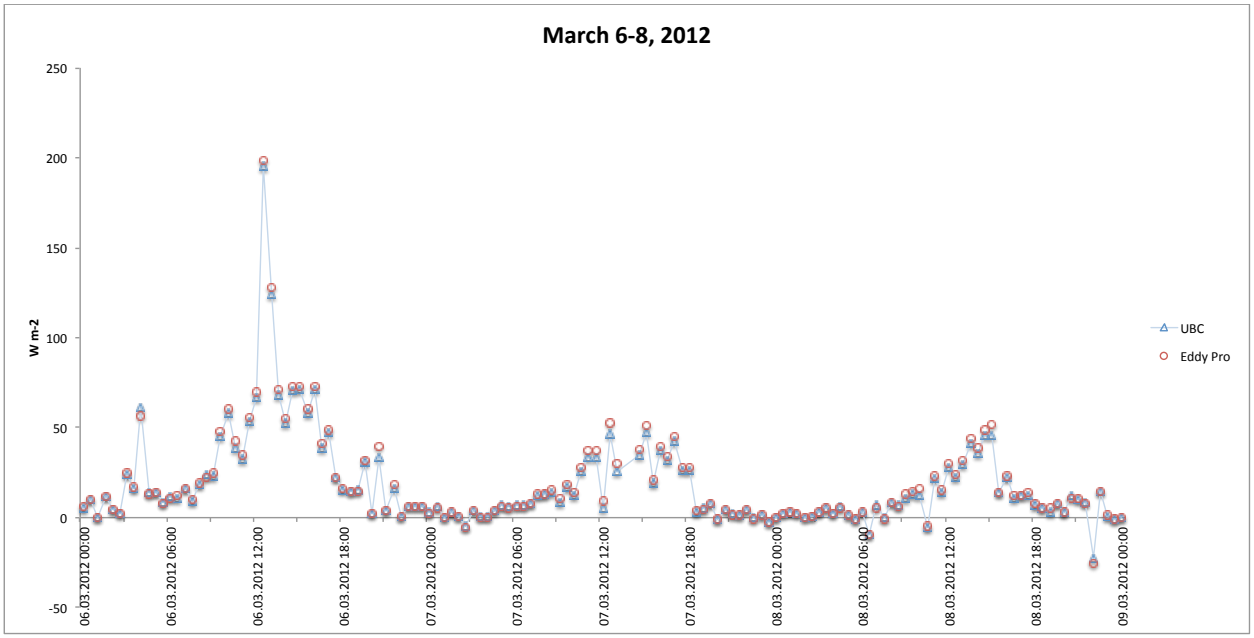

Figure 10 - *Time series of latent heat flux calculated using ubc_mmd.app (UBC, blue triangles) and Eddy Pro (red circles) for the three day period of March 6 to March 8, 2012.*

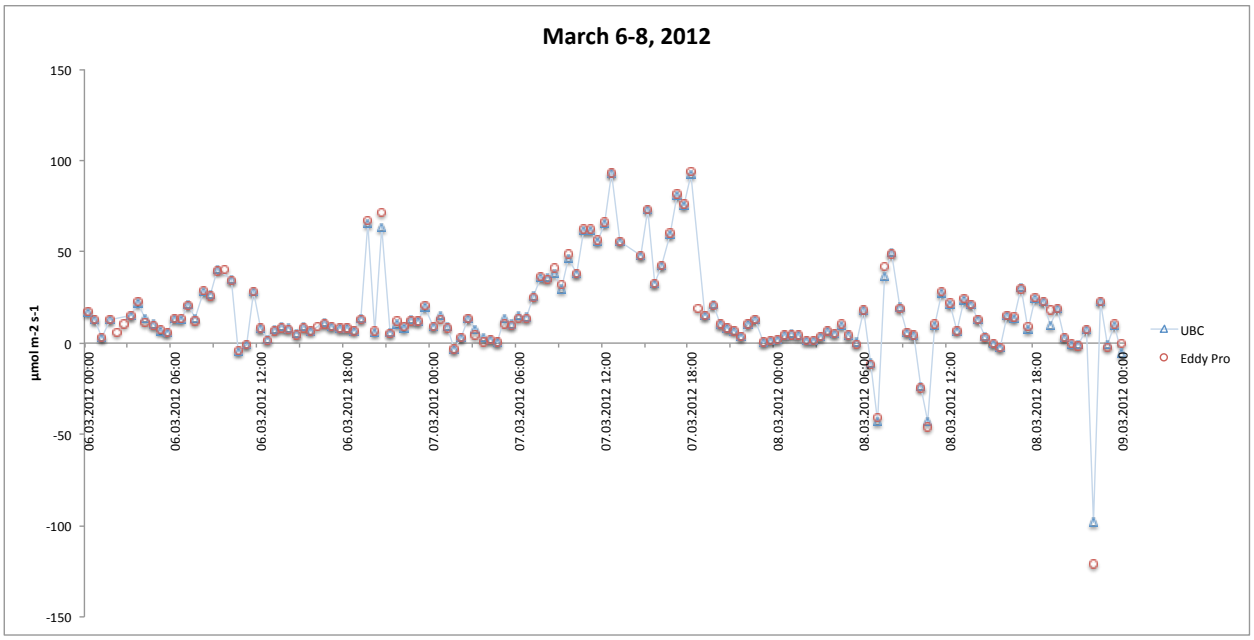

Figure 11 - *Time series of carbon-dioxide (CO_2) flux calculated using ubc_mmd.app (UBC, blue triangles) and Eddy Pro (red circles) for the three day period of March 6 to March 8, 2012.*

References

Campbell Scientific, Inc (2009). CSAT3 Instruction Manual, Revision 7/09. http://www.campbellsci.com/documents/manuals/csat3.pdf

LI-COR Inc. (2004). LI-7500 Instruction Manual, Revision 4. ftp://ftp.licor.com/perm/env/LI-7500/Manual/LI-7500Manual_V4.pdf

Christen A., van Gorsel E., Vogt R., M. Andretta and M. W. Rotach (2001): Ultrasonic Anemometer Instrumentation at Steep Slopes: Wind Tunnel Study - Field Intercomparison - Measurements. *MAP Newsletter 15*. 164-167

Finnigan, J.J., R. Clement, Y. Malhi, R. Leuning, and H.A. Cleugh (2002). A re-evaluation of long-term flux measurement techniques, Part I: Averaging and coordinate rotation. *Boundary-Layer Meteorology*, 107, 1-48.

Hollinger, D.Y., F.M. Kelliher, J.N. Byers, J.E. Hunt, T.M. McSeveny, P.L. Weir (1994) Carbon dioxide exchange between an undisturbed old-growth temperate forest and the atmosphere. *Ecology*, 75,.1, 134-150.

McMillen, R.T. (1988). An eddy correlation technique with extended applicability to non-simple terrain. *Boundary-Layer Meteorology*, 43, 231-245.

Moore, C.J. (1986). Frequency response corrections for eddy correlation systems. *Boundary-Layer Meteorology*, 37, 17-35.

Schotanus, P., F.T.M. Nieuwstadt, H.A.R. Bruin (1983). Temperature measurement with a sonic anemometer and its application to heat and moisture fluxes. *Boundary-Layer Meteorology*, 26, 81-93.

Vickers, D. and L. Mahrt (1997). Quality control and flux sampling problems for tower and aircraft data. *Journal of Atmospheric and Oceanic Technology*, 14, 512-526.

Webb, E.K., G.I. Pearman, and R. Leuning (1980). Correction of flux measurements for density effects due to heat and water vapour transfer. *Quarterly Journal of the Royal Meteorological Society*, 106, 85-100.